

# Peroxisome-Proliferator-Activated Receptor $\delta$ Activates Fat Metabolism to Prevent Obesity

Yong-Xu Wang,<sup>1</sup> Chih-Hao Lee,<sup>1,2</sup> Sambath Tiep,<sup>1</sup> Ruth T. Yu,<sup>1</sup> Jungyeob Ham,<sup>3</sup> Heonjoong Kang,<sup>3</sup> and Ronald M. Evans<sup>1,2,\*</sup>

<sup>1</sup>Gene Expression Laboratory

<sup>2</sup>Howard Hughes Medical Institute  
The Salk Institute

10010 North Torrey Pines Road  
La Jolla, California 92037

<sup>3</sup>Marine Biotechnology Laboratory  
Oceanography Program  
School of Earth and Environmental Sciences  
Seoul National University, NS-80  
Seoul 151-747  
Korea

## Summary

In contrast to the well-established roles of PPAR $\gamma$  and PPAR $\alpha$  in lipid metabolism, little is known for PPAR $\delta$  in this process. We show here that targeted activation of PPAR $\delta$  in adipose tissue specifically induces expression of genes required for fatty acid oxidation and energy dissipation, which in turn leads to improved lipid profiles and reduced adiposity. Importantly, these animals are completely resistant to both high-fat diet-induced and genetically predisposed (*Lepr<sup>db/db</sup>*) obesity. As predicted, acute treatment of *Lepr<sup>db/db</sup>* mice with a PPAR $\delta$  agonist depletes lipid accumulation. In parallel, PPAR $\delta$ -deficient mice challenged with high-fat diet show reduced energy uncoupling and are prone to obesity. In vitro, activation of PPAR $\delta$  in adipocytes and skeletal muscle cells promotes fatty acid oxidation and utilization. Our findings suggest that PPAR $\delta$  serves as a widespread regulator of fat burning and identify PPAR $\delta$  as a potential target in treatment of obesity and its associated disorders.

## Introduction

In western cultures, excess adipose mass, or obesity, has reached epidemic proportions, resulting in metabolic syndrome or syndrome X, typified by type 2 diabetes, cardiovascular disease, hypertension, and hyperlipidemia. In mammals, white fat and brown fat serve as major sites to control fatty acid metabolism and energy homeostasis (Lowell and Spiegelman, 2000; Spiegelman and Flier, 2001). White adipose stores energy in the form of triglycerides, which is released as free fatty acids in times of energy need, while brown adipose dissipates energy as heat by uncoupling ATP production from biochemical respiration. This energy dissipation process, termed adaptive thermogenesis, also occurs in skeletal muscle. While a set of uncoupling proteins (UCPs) on the mitochondrial inner membrane are the ultimate effectors for adaptive thermogenesis, they must coordinate with fuel oxidation, which generates the energy (electro-

chemical potential gradient) for subsequent heat conversion. Adaptive thermogenesis is a physiological defense against obesity (Lowell and Spiegelman, 2000; Spiegelman and Flier, 2001); however, at the transcriptional level, how this process is controlled, in particular how fuel oxidation and energy uncoupling is integrated, is not well understood.

Peroxisome proliferator-activated receptors (PPARs) are ligand-activated transcription factors belonging to the nuclear receptor superfamily (Kersten et al., 2000; Chawla et al., 2001b). They form obligate heterodimers with the retinoid X receptor and bind to defined PPAR elements in the promoter region of target genes. The PPAR subgroup comprises three closely related members: PPAR $\alpha$ ,  $\gamma$ , and  $\delta$ . They are activated by a variety of fatty acids, fatty acid derivatives, and synthetic compounds. Each member displays a tissue-selective expression pattern, with PPAR $\alpha$  and PPAR $\gamma$  predominantly in the liver and adipose tissue, respectively, and PPAR $\delta$  in many tissues. Genetic and pharmacological studies have revealed distinct roles of PPAR $\gamma$  and PPAR $\alpha$  in lipid metabolism. PPAR $\gamma$  serves as an essential regulator for adipocyte differentiation and promotes lipid storage in mature adipocytes by increasing the expression of several key genes in this pathway (Rosen and Spiegelman, 2001; Berger and Moller, 2002). These two important functions of PPAR $\gamma$  in adipocytes are suggested to largely account for the insulin sensitizing effects of the anti-diabetic thiazolidinediones (Yamauchi et al., 2001b). In contrast, PPAR $\alpha$  enhances fatty acid combustion in liver by upregulating genes encoding enzymes in  $\beta$ -oxidation and hence mediates the hypolipidemic effects of the fibrates (Reddy and Hashimoto, 2001; Berger and Moller, 2002). While this PPAR $\alpha$ -regulated  $\beta$ -oxidation pathway in the liver plays a major role in generating ketone bodies to support general fuel needs during fasting, similar mechanisms must exist within the peripheral tissues to enable local response to energy load and demands.

The functions of PPAR $\delta$  remain largely mysterious. Besides the demonstration of its critical role in epidermal maturation and skin wound healing (Michalik et al., 2001; Tan et al., 2001), recent studies have also linked this receptor to lipid metabolism. Synthetic PPAR $\delta$  agonists promote cholesterol accumulation in human macrophages (Vosper et al., 2001) and increase serum HDL while lowering triglyceride levels in obese animal models (Leibowitz et al., 2000; Oliver et al., 2001). Interestingly, although the large percent of PPAR $\delta$  null mutant mice are embryonically lethal due to placental defects, the small number of mice that do survive show decreased adiposity (Peters et al., 2000; Barak et al., 2002). However, no reduction of fat mass is observed in adipose-specific ablation of PPAR $\delta$  mice (Barak et al., 2002), indicating a complex, nonautonomous action. These data collectively implicate PPAR $\delta$  in lipid homeostasis; but which metabolic pathway it regulates in vivo and whether it functionally overlaps with PPAR $\gamma$  or PPAR $\alpha$  remain unclear.

In an attempt to pinpoint the in vivo functions of

\*Correspondence: [evans@salk.edu](mailto:evans@salk.edu)

PPAR $\delta$ , we undertook a gain-of-function approach by selectively expressing an active form of PPAR $\delta$  in adipose tissue. The resulting transgenic mice display decreased lipid accumulation in both adipose tissue and serum. The mice are lean and are protected from obesity. Additionally, short-term treatment of obese mice with PPAR $\delta$  agonist causes a dramatic lipid depletion in tissues. These phenotypes are consistent with an elevated energy expenditure. Indeed, we find that PPAR $\delta$  activates an array of genes required for fatty acid combustion and uncoupling, but not that of genes involved in lipogenesis and storage, which are controlled by PPAR $\gamma$ . Furthermore, PPAR $\delta$ -deficient mice fed with high-fat diet display reduced energy uncoupling and are prone to obesity. In corroboration with these *in vivo* findings, we demonstrate that activation of PPAR $\delta$  stimulates  $\beta$ -oxidation and triglyceride utilization in adipocytes and myocytes. Our data suggest that PPAR $\delta$  is a key regulator of fat burning in peripheral tissues by coordinating fatty acid oxidation and energy uncoupling.

## Results

### Activation of PPAR $\delta$ in Adipose Tissue Decreases Fat Mass and Lipid Accumulation

We fused the 78 amino acid VP16 activation domain of the herpes simplex virus to the N-terminal end of PPAR $\delta$ . In cell transfection assays, this fusion protein (VP16-PPAR $\delta$ ) shows potent ligand-independent transactivation on our synthetic pan-PPAR response element, but not on the response elements of other nuclear receptors (data not shown). Like wild-type PPAR $\delta$ , VP16-PPAR $\delta$  has no effect on a reporter containing a native PPAR $\gamma$ -specific response element we identified recently (Y. Barak and R.M.E., unpublished data), suggesting that VP16-PPAR $\delta$  has no altered promoter selectivity. We expressed VP16-PPAR $\delta$  in adipose tissue under the control of the enhancer-promoter region of the adipocyte fatty acid binding protein (aP2) gene (Ross et al., 1990). Three transgenic founders *a*, *b*, and *c* were obtained, which are distinguishable from their littermates due to a marked reduction in body weight and adiposity (Figure 1). Founder *a* represents the most severe case and lacks any visible white fat. This fatless phenotype resembles that of lipotrophic mice caused by defects in adipogenesis (Moitra et al., 1998; Shimomura et al., 1998; Barak et al., 1999). However, none of these lines including founder *a* exhibit other features of lipotrophic mice, such as hypertriglyceridemia, enlarged viscera, or fatty liver (Figure 1A and data not shown). These distinctions argue against an adipogenesis defect and raise the possibility that the fat pad in our transgenic mice may have increased fatty acid consumption, thereby precluding significant storage in either liver or other organs. Founder *b* and *c* show similar reduction in fat pad size (Figure 1B and see Figure 3D), and based on reproductive competency (normal size litters and expected ratio of transgene), a cohort was expanded from the *c* male.

We estimated that there are 2–3 copies of the transgene present in the genome (Figure 2A). The transgene is expressed in both white fat and brown fat but is absent in other tissues, as shown by Western blot analysis with

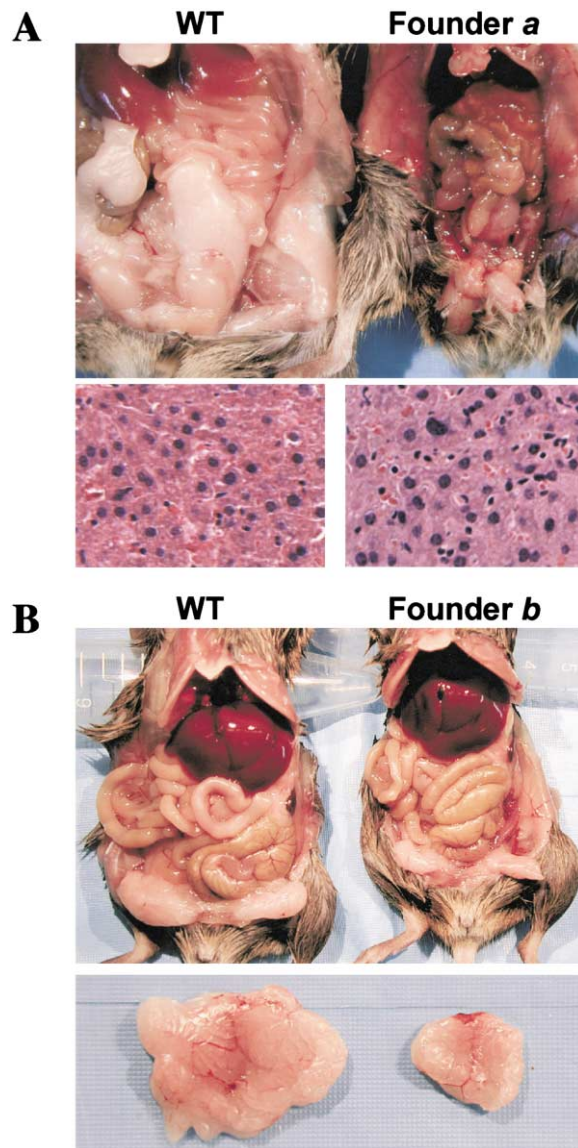


Figure 1. Reduced Adiposity in VP16-PPAR $\delta$  Transgenic Mice without Lipid Accumulation in Other Tissues

(A) (Top image) A ventral view of founder *a* and its control littermate. Note the complete loss of reproductive fat in the transgenic mouse. (Lower image) H&E stained sections of liver from founder *a* and its control littermate.

(B) (Top image) A ventral view of founder *b* and its control littermate. (Lower image) A comparison of reproductive fat pads. Founder *c* exhibits essentially the same reduced fat phenotype as founder *b*.

anti-PPAR $\delta$  and anti-VP16 antibodies (Figures 2B and 2C). Compared to that of endogenous PPAR $\delta$ , the level of VP16-PPAR $\delta$  protein is lower in white fat (WAT), but is similar or slightly higher in brown fat (BAT). Adipocyte-differentiation-related protein (ADRP) is a lipid droplet coating protein and its expression is induced by PPAR $\delta$  activation (Vosper et al., 2001). Indeed, Northern blot analysis revealed a 3-fold increase of ADRP gene expression in the brown fat of transgenic mice, confirming that the VP16-PPAR $\delta$  is functional *in vivo* (Figure 2D). Interestingly, we did not observe a significant induction

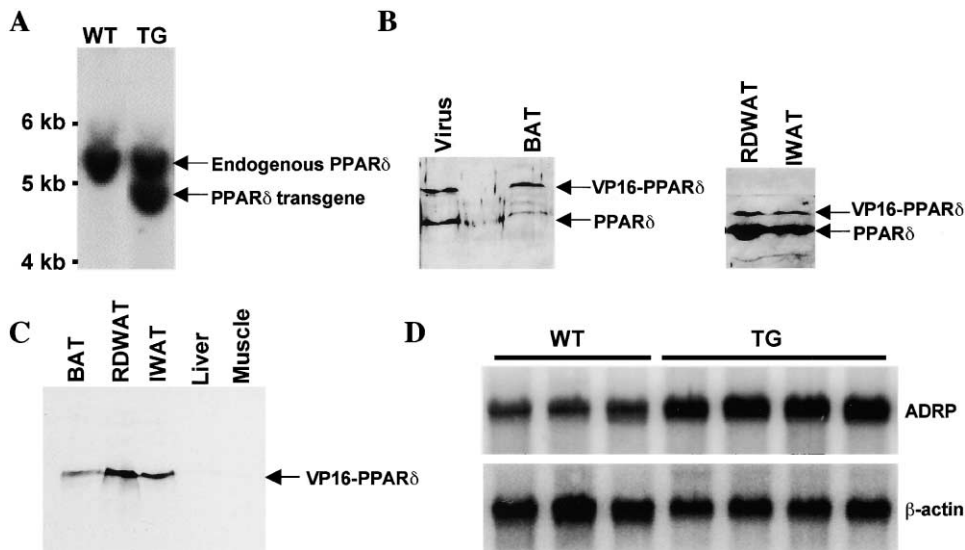


Figure 2. Expression and Functional Verification of the VP16-PPAR $\delta$  Transgene

(A) Southern blot analysis. Genomic tail DNA (20  $\mu$ g/lane) from wild-type (WT) and transgenic (TG) mice was digested with HindIII/EcoRV, separated on agarose gel, and probed with PPAR $\delta$  cDNA.  
 (B) Protein extracts from brown fat (BAT), reproductive fat (RDWAT), and inguinal fat (IWAT) were assayed for PPAR $\delta$  and VP16-PPAR $\delta$  by Western blot analysis with PPAR $\delta$  antibodies. Lane 1 (virus) was loaded with protein extracts generated from 3T3-L1 cells infected with PPAR $\delta$  and VP16-PPAR $\delta$  adenovirus to show the position of the two proteins. Note, for reasons unclear, PPAR $\delta$  and VP16-PPAR $\delta$  from adipose tissue migrate slower than from 3T3-L1 cells and higher amount of PPAR $\delta$  is retained on the top portion of the gel than that of VP16-PPAR $\delta$  (not shown), thus the protein levels of PPAR $\delta$  and VP16-PPAR $\delta$  in brown fat are approximately equal.  
 (C) Protein extracts from BAT, RDWAT, IWAT, liver, and muscle were assayed for VP16-PPAR $\delta$  by Western blot analysis with VP16 antibodies. Each lane was loaded with equivalent weight of tissues.  
 (D) Total RNA (10  $\mu$ g/lane) from brown fat of 3 control littermates (WT) and 4 transgenic mice (TG) was analyzed by Northern blot with probes for ADRP and  $\beta$  actin.

of ADRP in white fat, indicating that target gene regulation by PPAR $\delta$  is highly tissue or cell-type-selective.

On a standard diet, despite a daily food intake similar to that of control littermates when measured in individually housed mice (Figure 3A), the transgenic mice are about 20% smaller in body weight at 4 months old, and this difference is increased to 35% at 12 months old (Figure 3B). In contrast, transgenic expression of the VP16 activation domain alone in adipose tissue (aP2-VP16) produces no discernable differences relative to control nontransgenic littermates in body weight, physiology, or histology (Figure 3C and data not shown). We measured the weight of various tissues normalized by body weight in VP16-PPAR $\delta$  transgenic mice. There is a 40% decrease in the reproductive white fat depot (Figure 3D). This is in marked contrast to other tissues including brown fat, liver, heart, and kidney, which have weights similar to wild-type and exhibit no gross abnormalities. Adipose tissues, but not other tissues, show striking morphological changes (Figure 3E). In control littermates, white fat adipocytes are uniform in size, whereas in transgenic mice, adipocytes, especially for inguinal and retroperitoneal fat depots, are smaller and heterogeneous in size, indicating that the reduction in total fat mass may result from less triglyceride accumulation rather than a reduced number of adipocytes. Reduction of lipid accumulation is even more prominent in brown fat. Brown fat adipocytes normally contain multiple lipid droplets. Both the number and the size of lipid droplets are reduced in transgenic mice. To deter-

mine whether the reduced fat weight and lipid accumulation occur at the expense of lipid buildup in the circulation, we assayed serum lipid levels. While levels of total cholesterol remain unchanged, those of total triglyceride and free fatty acid are significantly decreased (Figure 3F). These results, together with the lack of lipid accumulation in liver and muscle, are consistent with our hypothesis that activation of PPAR $\delta$  in adipose promotes fatty acid consumption.

#### Activation of PPAR $\delta$ in Adipose Protects against Obesity and Hyperlipidemia

In principle, enhanced fatty acid utilization should protect mice against high-fat diet induced obesity. Accordingly, we challenged 8-week-old mice with a high-fat diet containing 35% (w/w) fat for 32 days to stimulate weight gain. As shown in Figure 4A, weight gain is highly blunted in the transgenic mice relative to the control littermates. A statistical difference is observed as early as the first two weeks of feeding. By the end of this feeding period, the control littermates have become mildly obese ( $38.60 \pm 0.85$  g, and Figure 4B), while the transgenic mice still weigh slightly less than chow diet-fed nontransgenic mice ( $24.46 \pm 0.64$  versus  $26.84 \pm 0.37$  g). The net weight gains are  $5.27 \pm 0.61$  g and  $12.40 \pm 0.76$  g, respectively, for transgenic and control littermates fed with the high-fat diet. The body weight difference is largely due to the difference in fat mass. The inguinal, reproductive, and retroperitoneal fat depots each weigh one-third of that of control littermates,

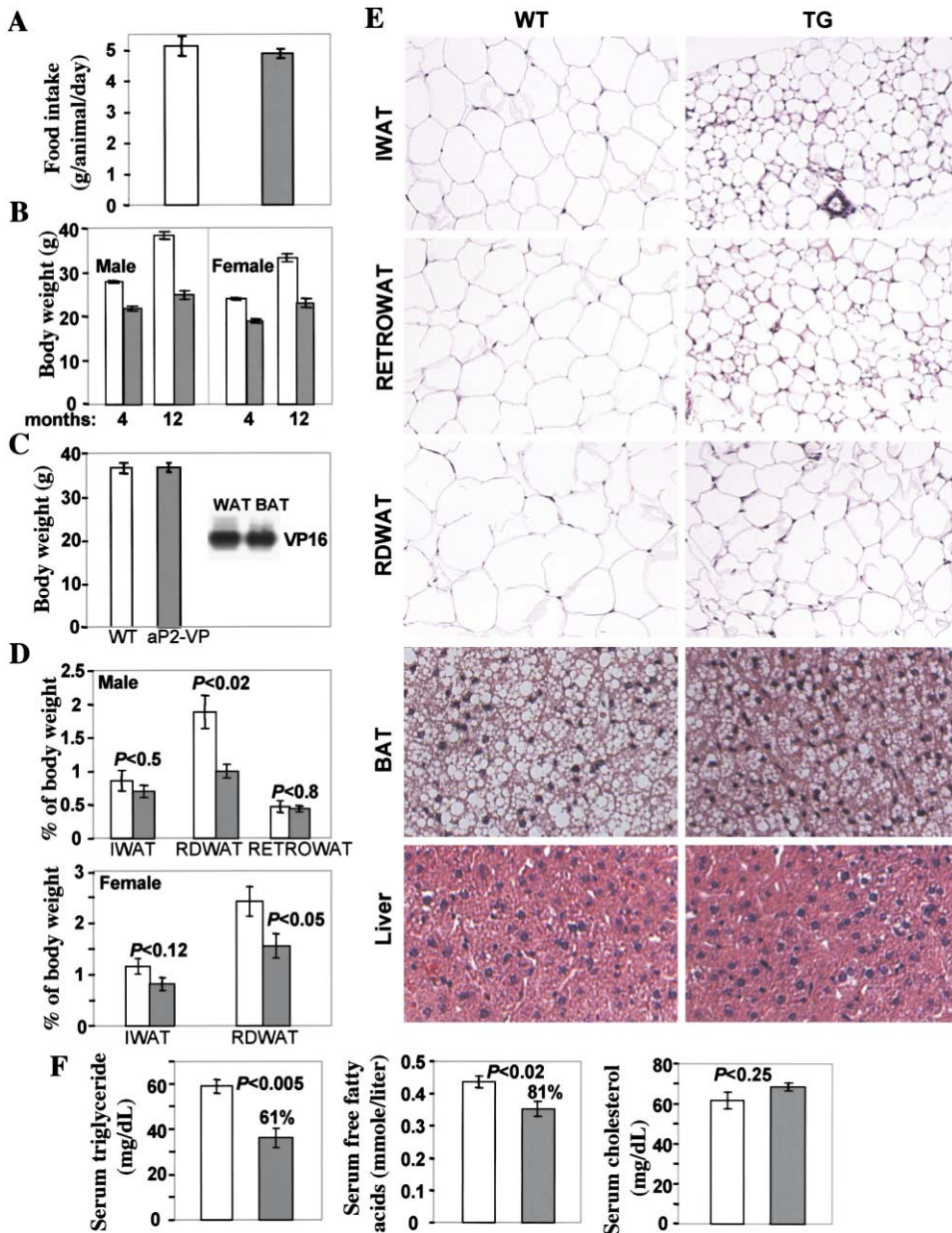


Figure 3. Phenotypes of the Transgenic Mice

(A) Food intake measured over 15 days in individually housed four-month-old male mice ( $n = 7-11$ ). Food intake was averaged for each mouse and then averaged for each group.  
 (B) Body weights of four-month-old mice ( $n = 6$  for male;  $n = 5-6$  for female), and of twelve-month-old mice ( $n = 9-14$  for male;  $n = 6-8$  for female).  
 (C) Body weights of eleven-month-old male aP2-VP16 transgenic mice and their nontransgenic littermates ( $n = 8$ ). No body weight difference was observed in female mice either. The expression of VP16 transgene in adipose was shown by northern analysis.  
 (D) Weights of white fat depots normalized by body weight at seven and five months of age, respectively, for male ( $n = 5-6$ ) and female ( $n = 5-6$ ) mice.  
 (E) Histology of adipose tissue of the transgenic mice. Sections from inguinal fat (IWAT), retroperitoneal fat (RETROWAT), reproductive fat (RDWAT), brown fat (BAT), and liver were stained with H&E.  
 (F) Steady-state serum levels of triglycerides ( $n = 4-6$ ), free fatty acids ( $n = 5-6$ ), and total cholesterol ( $n = 4-6$ ). Five-month-old female mice. Empty bar, wild-type; filled bar, transgenic.

and only one-half when normalized by body weight (Figure 4C). While high-fat feeding increases serum triglyceride and free fatty acid levels by 2-fold in control littermates, activation of PPAR $\delta$  in adipose results in a lipid profile close to that of wild-type mice under the standard chow diet (Figure 4D, compare to Figure 3F).

As expected, high-fat feeding causes adipocyte hypertrophy and massive lipid accumulation in both white fat and brown fat in control littermates, while little, if any, of these changes are found in transgenic mice (Figure 4E, and data not shown). Moreover, nontransgenic mice develop fatty liver, suggesting a saturated lipid storage

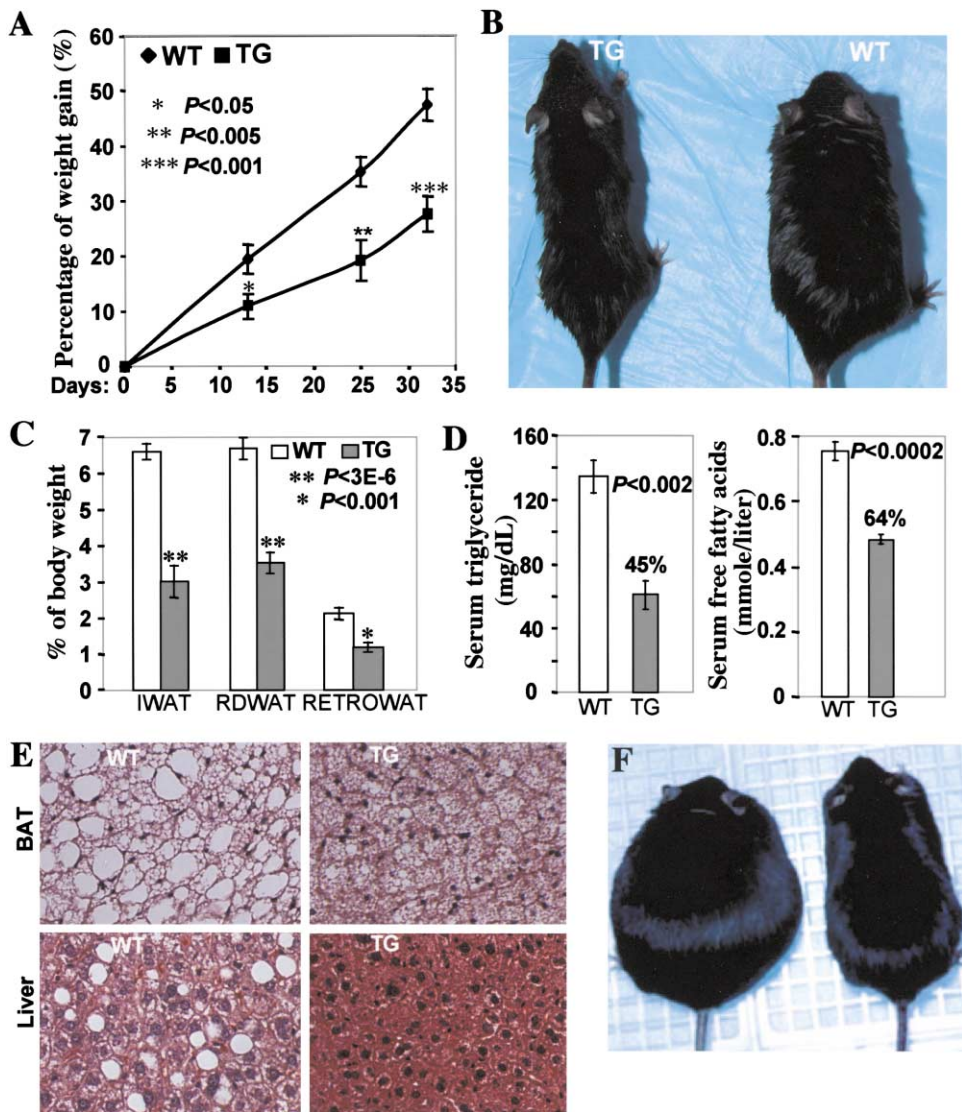


Figure 4. Activation of PPAR $\delta$  in Adipose Tissue Protects from Obesity and Hyperlipidemia

(A) Eight-week-old male mice ( $n = 6-7$ ) were fed with a high-fat diet. The increases in body weights were calculated based on the initial body weight at day 0 of high-fat feeding. The initial body weights are  $19.20 \pm 0.46$  g for transgenic mice, and  $26.20 \pm 0.24$  g for control littermates. (B) Photographs of representative control littermate and transgenic mice after five weeks of high-fat diet feeding. (C) Weights of white fat depots normalized by body weight ( $n = 7-9$ ). (D) Steady-state serum levels of triglycerides ( $n = 4$ ) and free fatty acids ( $n = 4$ ). Serum levels of total cholesterol were not assayed. (E) Prevention of lipid accumulation in adipose tissue and liver. Sections of brown fat and liver were stained with H&E. (F) Photographs of representative *Lep<sup>db/db</sup>* (Left) and *Lep<sup>db/db</sup>/VP16-PPAR $\delta$*  (Right) mice.

in adipose. However, no appreciable fatty acid accumulation in liver is observed in transgenic mice (Figure 4E). Thus activation of PPAR $\delta$  in adipose, possibly via increasing energy expenditure, counteracts high-fat-induced obesity, and prevents fatty liver and hyperlipidemia.

We next examined whether activation of PPAR $\delta$  in adipose tissue can protect a genetically fat model, *Lep<sup>db/db</sup>* mice, from developing obesity. *Lep<sup>db/db</sup>* mice exhibit markedly increased adiposity due to hyperphagia caused by mutation in the leptin receptor gene (Chen et al., 1996; Lee et al., 1996). We obtained *Lep<sup>db/db</sup>* mice harboring the transgene. At 5 weeks, the body weight differences between *Lep<sup>db/db</sup>* and *Lep<sup>db/db</sup>/VP16-PPAR $\delta$*  mice are distinguishable. The body weight differences

continue to increase with age. At 16 weeks, *Lep<sup>db/db</sup>* mice are overtly obese and weigh  $54.46 \pm 1.26$  g ( $n = 6$ ), while *Lep<sup>db/db</sup>/VP16-PPAR $\delta$*  mice only weigh  $31.70 \pm 1.35$  g ( $n = 5$ ) (Figure 4F), which is close to that of their control littermates ( $33.86 \pm 1.80$  g,  $n = 5$ ). These results demonstrate that activation of PPAR $\delta$  in adipose reverses the obesity phenotype of *Lep<sup>db/db</sup>* mice and also suggest that the anti-obesity function of PPAR $\delta$  does not require the presence of leptin signaling pathway.

#### PPAR $\delta$ Agonist Depletes Tissue Lipid Storage in *Lep<sup>db/db</sup>* Mice

We extended our in vivo studies of *Lep<sup>db/db</sup>* mice using a PPAR $\delta$  specific agonist, GW501516 (Oliver et al., 2001). Age- and weight-matched *Lep<sup>db/db</sup>* mice were treated

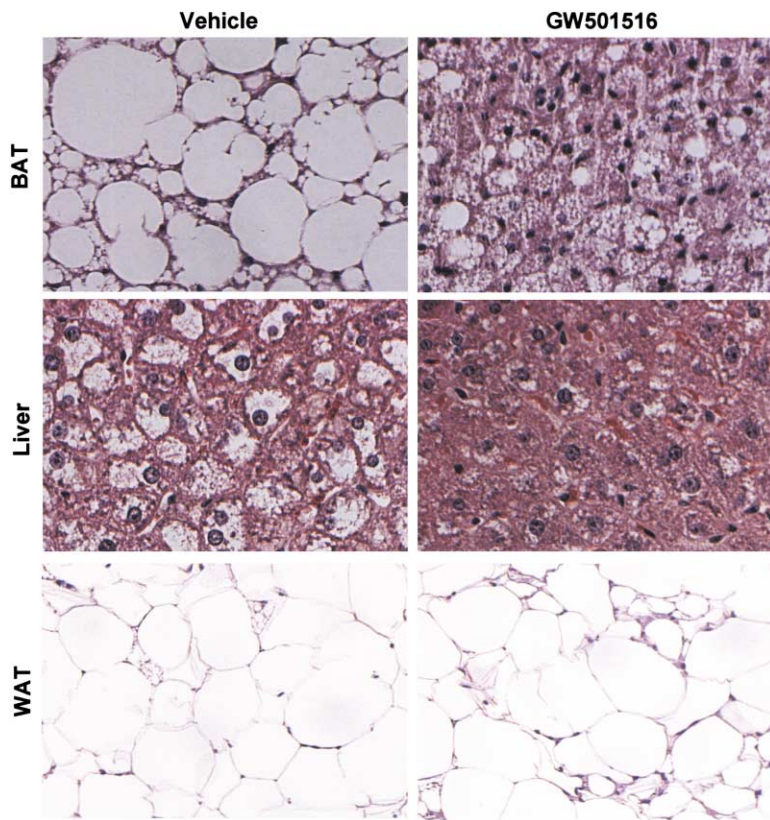


Figure 5. PPAR $\delta$  Agonist Rapidly Depletes Lipid Accumulation of Brown Fat and Liver in *Lepr<sup>db/db</sup>* Mice

Age- and weight-matched *Lepr<sup>db/db</sup>* mice were treated with vehicle or GW501516 for 7 days. Sections of brown fat, liver, and inguinal fat were then stained with H&E.

with vehicle or GW501516 for 7 days. We then examined the histology of brown fat and liver, since these two tissues accumulate unusual amounts of lipids in *Lepr<sup>db/db</sup>* mice. As shown in Figure 5, brown fat in vehicle-treated *Lepr<sup>db/db</sup>* mice resembles white fat, each cell filled with a single massive lipid droplet, pushing the nucleus to the cell periphery. Remarkably, in GW501516 treated *Lepr<sup>db/db</sup>* mice, brown fat adipocytes show increased mitochondria-rich eosinophilic staining, disappearance of large lipid droplets, and replacement with multiple small droplets. Thus, even a relatively short-term agonist treatment leads to a rapid restoration of brown fat appearance with reduced lipid content and enhanced metabolic activity. As might be predicted, a vast reduction of lipid accumulation in the liver was also found (Figure 5). We did not see significant histological changes of white fat, presumably due to the very short period of treatment. These observations essentially mirror the phenotypes in the transgenic mice fed with high-fat diet, reaffirming the role of PPAR $\delta$  activation in fatty acid metabolism.

#### PPAR $\delta$ Selectively Activates Genes of Fatty Acid Oxidation and Energy Uncoupling

The data presented above indicate an upregulation of fatty acid combustion by activation of PPAR $\delta$ . We sought to understand the molecular basis underlying this metabolic change. We compared the expression of genes involved in fatty acid metabolism by Northern blot and phosphorimager analysis (Figures 6A and 6B). Brown fat is the major tissue for adaptive thermogenesis that dissipates energy as heat via uncoupling protein

UCPs. All three UCPs are expressed in brown fat with UCP1 being most abundant. Activation of PPAR $\delta$  induces expression of UCP1 and UCP3 in brown fat by 3.0- and 2.8-fold, respectively, but has no effect on the expression of UCP2. We next examined the expression of genes encoding enzymes for fatty acid  $\beta$ -oxidation. Long chain acyl-CoA synthetase (LCAS; 2.2-fold), very long chain acyl-CoA synthetase (VLCAS; 2.1-fold), acyl-CoA oxidase (AOX; 2.0-fold), the muscle form of carnitine palmitoyltransferase-1 (mCPT1; 1.7-fold), long chain acyl-CoA dehydrogenase (LCAD; 1.7-fold), and very long chain acyl-CoA dehydrogenase (VLCAD; 1.9-fold) are all upregulated in brown fat. Interestingly, these oxidation genes have previously been found to be induced by PPAR $\alpha$  agonists in the liver (Reddy and Hashimoto, 2001; Berger and Moller, 2002). We also observed a mild but significant induction of hormone-sensitive lipase (HSL; 1.7-fold), which catalyzes triglyceride hydrolysis in adipocytes. Surprisingly, activation of PPAR $\delta$  causes no significant changes for genes involved in lipogenesis (SREBP1) and lipid storage (CD36 and aP2), which are induced by PPAR $\gamma$  agonists in adipose tissue (Yamauchi et al., 2001b; Berger and Moller, 2002). Expression of adipocyte-secreted proteins, ACRP30 and resistin, which are also regulated by PPAR $\gamma$  and are implicated in fatty acid and glucose metabolism (Berg et al., 2001; Stepan et al., 2001; Yamauchi et al., 2001a), remains unchanged. In white fat, we observed no difference for most of these genes, except for UCP1, which shows a robust induction (Figure 6B). UCP1 is the hallmark for brown fat. The ability of PPAR $\delta$  to promote a brown fat-like feature of white fat is reminiscent of that of the

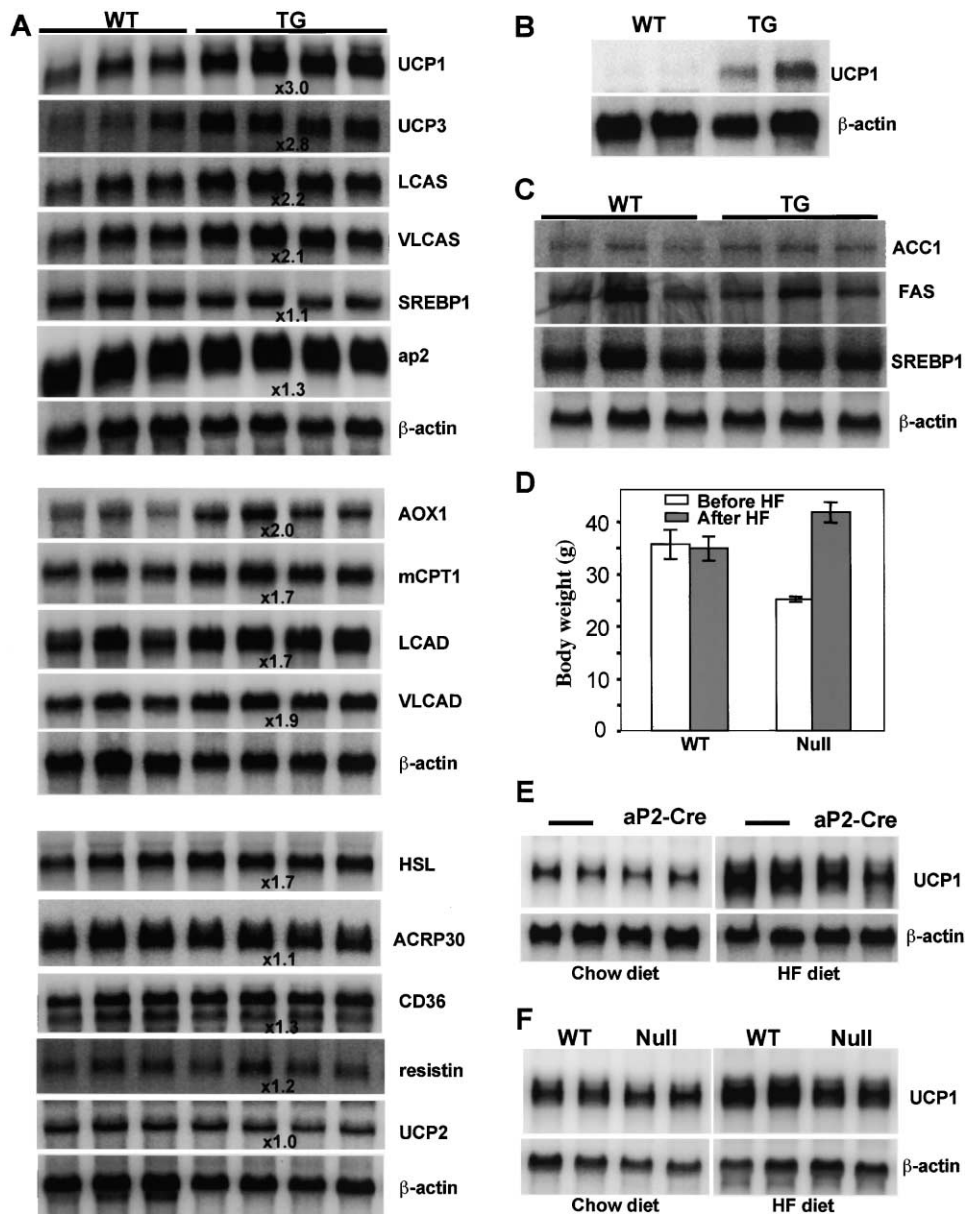


Figure 6. PPAR $\delta$  Activates Genes Required for Oxidation and Thermogenesis in Adipose Tissue

(A–C) Northern blot analysis of gene expression in brown fat (A), white fat (B), and liver (C) of the transgenic mice. Total RNA (10  $\mu$ g/lane) was hybridized with indicated probes. Intensity of the signals was quantitated by phosphorimager analysis and the fold induction in the transgene was calculated after normalization with  $\beta$  actin signal. Full names of the probes used are found in the text.

(D) PPAR $\delta$  null is prone to high-fat-induced obesity. Eight-month-old male PPAR $\delta$  null mice were fed with chow diet or high-fat diet for 3 weeks.

(E) Male-floxed PPAR $\delta$  mice with or without aP2-CRE were fed with high-fat diet for 1 week. RNA was isolated from brown fat and hybridized with UCP1 probe.

(F) RNA from brown fat of mice used in (D) was isolated and analyzed for UCP1 expression.

transcriptional coactivator PGC-1 $\alpha$  (Puigserver et al., 1998); however, no upregulation of PGC-1 $\alpha$  is found in either white fat or brown fat of the transgenic mice (data not shown). Although the level of UCP1 induced by PPAR $\delta$  in white fat is low relative to that in brown fat, its functional significance cannot be excluded, given the large quantity of white fat. Indeed, low levels of transgenic UCP1 expression in white fat are sufficient to protect against obesity (Kopecky et al., 1996). In ag-

gregate, our gene expression data reveal that PPAR $\delta$  activates each of the three steps of fatty acid catabolism in brown fat: hydrolysis, oxidation, and uncoupling of oxidative phosphorylation. The ability of PPAR $\delta$  activation to prevent high-fat-induced fatty liver raised the possibility that this might be due to an indirect effect on fatty acid synthesis in liver. An examination of the expression levels of acetyl-CoA carboxylase 1 (ACC1), fatty acid synthase (FAS), and SREBP1 in the liver re-

veals no obvious differences of transgenic mice and control littermates (Figure 6C). These results suggest that the observed phenotypes are indeed direct consequences of activated metabolism in adipose tissue.

Having established that PPAR $\delta$  acts as a thermogenic transcriptional factor, we reasoned that ablation of PPAR $\delta$  should constrain the oxidative response, resulting in increased body weight gain upon energy overload. As previously reported, PPAR $\delta$  null mice are runted at birth and during the first 12 months and weigh much less than wild-type mice under normal chow diet. However, when placed on a high-fat diet, they gain weight rapidly and their body weights surpass those of wild-type mice after a 3 weeks trial ( $41.8 \pm 1.97$  g versus  $34.9 \pm 2.34$  g,  $n = 6$ ,  $P < 0.05$ ; Figure 6D). In contrast, during this feeding period, age-matched PPAR $\delta$  null mice under chow diet or age-matched wild-type mice under either chow diet or high-fat diet show little weight changes. We also observed that PPAR $\delta$  null mice accumulate much higher amount of lipids in brown fat than controls under high-fat diet (data not shown). We then examined UCP1 expression in brown fat of both adipose-specific PPAR $\delta$  knockout and null mice (Barak et al., 2002). Under normal chow diet, levels of UCP1 are similar between floxed PPAR $\delta$  mice (controls) and floxed PPAR $\delta$  mice with aP2-CRE (knockouts). Whereas UCP1 is robustly induced after 1 week high-fat feeding in control animals, the induction is significantly compromised in knockouts (Figure 6E). Similar decrease of UCP1 expression is observed in PPAR $\delta$  null mice fed with high-fat diet (Figure 6F). Thus, under conditions of high-fat diet, loss of PPAR $\delta$  in adipose tissue or in the whole animal results in impaired thermogenesis, partially explaining the rapid weight gain of null mice.

#### PPAR $\delta$ Stimulates Fatty Acid Oxidation in Cultured Adipocytes and Myocytes, and Associates with the Thermogenic Cofactor PGC-1 $\alpha$ In Vivo

We asked whether the function of PPAR $\delta$  could be recapitulated in vitro. In vivo studies with activated PPAR $\delta$  described here and adipose-specific PPAR $\delta$  ablation (Barak et al., 2002) suggest that PPAR $\delta$  is not involved in adipogenesis. In support of the in vivo data, we found no inhibitory or stimulatory effects of PPAR $\delta$  on 3T3-L1 adipocyte differentiation (data not shown). We next determined whether overexpression of PPAR $\delta$  promotes triglyceride consumption (Figures 7A and 7B). Preadipocytes were allowed to reach a fully differentiated state with triglyceride accumulation and then infected with virus expressing PPAR $\delta$  or VP16-PPAR $\delta$ . We assayed the levels of glycerol released into culture medium as an indicator of triglyceride metabolism. As shown in Figure 7A for a 6 hr time point, overexpression of PPAR $\delta$  leads to a 2-fold increase in glycerol release. This increase is due to activation of PPAR $\delta$  by intracellular fatty acids as endogenous ligands. Indeed, addition of the more potent PPAR $\delta$  selective agonist GW501516 further enhances the production of glycerol. Overexpression of VP16-PPAR $\delta$  results in a 3-fold production. A similar fold induction is observed over a 46 hr time point, with correspondingly increased glycerol levels in the medium (data not shown). We also measured total intracellular triglyceride levels following virus infection.

In agreement with increased glycerol release, the amount of total triglyceride in cells decreases significantly (Figure 7B). Moreover, we observed no difference in the levels of free fatty acids in the media between control and PPAR $\delta$  or VP16-PPAR $\delta$  overexpression experiments (data not shown), suggesting that the free fatty acids derived from triglyceride hydrolysis are effectively burned.

To determine whether endogenous PPAR $\delta$  promotes fatty acid utilization and to provide direct evidence that PPAR $\delta$  acts upon the  $\beta$ -oxidation pathway, we measured the level of  $\beta$ -oxidation in 3T3-L1 preadipocytes. Remarkably, while agonists for PPAR $\alpha$  (WY14643) or PPAR $\gamma$  (BRL49653) have little effect, PPAR $\delta$  agonist GW501516 stimulates  $\beta$ -oxidation by 50%, demonstrating that activation of endogenous PPAR $\delta$  is sufficient to increase fatty acid combustion (Figure 7C). Basal  $\beta$ -oxidation is increased by overexpressing PPAR $\delta$ , and addition of GW501516 or overexpression of VP16-PPAR $\delta$  results in a 2-fold increase (Figure 7D). In contrast, overexpression of PPAR $\gamma$  plus its agonist BRL49653 has only a marginal effect on  $\beta$ -oxidation, consistent with distinct functions for individual PPAR isoforms.

We next investigated whether PPAR $\delta$  can play a similar role in fatty acid catabolism and uncoupling in skeletal muscle. C2C12 cells were differentiated into myotubes and then treated with PPAR agonists. Consistent with our observations in adipocytes, the PPAR $\delta$  agonist GW501516 significantly increases fatty acid oxidation in myotubes, with no effects found for either PPAR $\alpha$  or PPAR $\gamma$  agonists (Figure 7E). Activation of ectopically expressed PPAR $\delta$  in myotubes leads to a much more robust stimulation (Figure 7E). Again, activation of ectopically expressed PPAR $\gamma$  produces little effect. In agreement with the oxidation data, the GW501516 compound induces the expression of genes required for fatty acid oxidation and uncoupling, while little or no induction is observed for PPAR $\alpha$  or PPAR $\gamma$  agonists (Figure 7F). Conversely, GW501516 treatment has no effects on genes for lipogenesis or fatty acid transport (Figure 7F). These in vitro results, together with our in vivo gene expression data, clearly demonstrate that PPAR $\delta$  controls fatty acids metabolism by promoting  $\beta$ -oxidation and energy uncoupling in peripheral tissues. Our results also indicate that, unlike PPAR $\delta$ , PPAR $\gamma$  and PPAR $\alpha$  have very limited thermogenic roles in both adipose and skeletal muscle.

The thermogenic function of PPAR $\delta$  described here is remarkably similar to that of the transcriptional coactivator PGC-1 $\alpha$ , raising the possibility that PGC-1 $\alpha$  acts through PPAR $\delta$  to promote thermogenesis. Indeed, in 293 cells overexpressing PPAR $\delta$  and PGC-1 $\alpha$ , coimmunoprecipitation studies reveal a strong physical interaction between these two proteins (Figure 7G). This interaction is enhanced by addition of GW501516 and critically depends on the LXXLL receptor interaction motif located between amino acids 142–146 of PGC-1 $\alpha$ . A residual interaction exists in the LXXLL motif mutant (LxxAA), but, unexpectedly, disappears in the presence of the PPAR $\delta$  agonist. In agreement with the interaction data, PGC-1 $\alpha$ , even in the absence of agonist, is a powerful coactivator for PPAR $\delta$  in transient transfection reporter assays of C2C12 muscle cells (Figure 7H). In contrast, the coactivator p300, the p160 family member ACTR, or the LXXLL mutant of PGC-1 $\alpha$  is inactive. Fi-



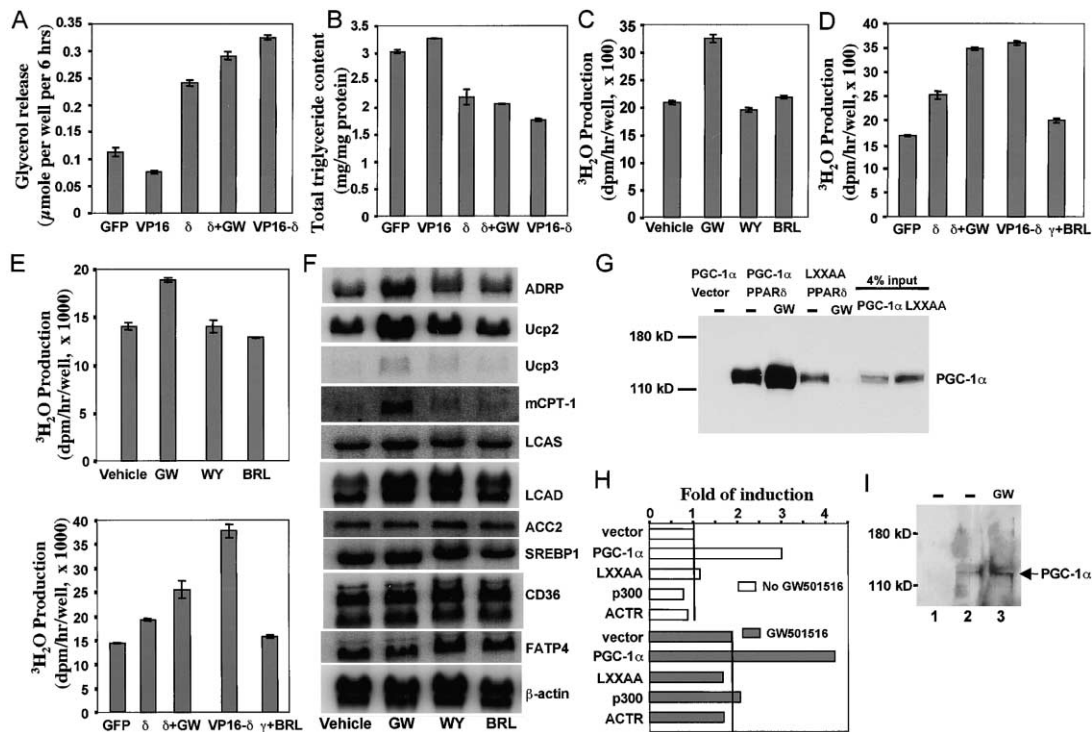


Figure 7. PPAR $\delta$  Promotes Fatty Acid  $\beta$ -Oxidation and Utilization in Adipocytes and Myotubes, and Associates with the Thermogenic Cofactor PGC-1 $\alpha$

(A) Triglyceride breakdown. Fully differentiated 3T3-L1 cells were infected with adenovirus expressing GFP, VP16, PPAR $\delta$  ( $\delta$ ), or VP16-PPAR $\delta$  (VP16- $\delta$ ) overnight. Cells were then washed and serum-starved overnight with or without GW501516 (GW) ligand (0.1  $\mu$ M). The next day cells were washed again and incubated with the serum-free medium for 6 hr. Glycerol released into the medium was assayed.

(B) Four days postvirus infection, adipocytes were lysed and levels of total triglycerides assayed.

(C and D)  $\beta$ -oxidation in adipocytes. (C) 3T3-L1 preadipocytes two day postconfluence were incubated with ligands GW501516 (0.1  $\mu$ M), WY14643 (WY) (15  $\mu$ M), or BRL49653 (BRL) (1  $\mu$ M) overnight, or (D) 3T3-L1 preadipocytes were infected with indicated adenovirus with or without indicated ligands (0.1  $\mu$ M for GW501516, 1  $\mu$ M for BRL) overnight. Next day cells were changed to serum-free medium containing  $^3\text{H}$ -palmitic acids.  $^3\text{H}_2\text{O}$  production was assayed 7 hr after incubation.

(E)  $\beta$ -oxidation in myotubes. Differentiated C2C12 muscle cells were treated as above.  $^3\text{H}_2\text{O}$  production was assayed 4 hr after incubation. Data were from quadruplicates.

(F) Target gene expression in myotubes. Myotubes were treated with vehicle, GW501516 (0.1  $\mu$ M), WY14643 (15  $\mu$ M), or BRL49653 (1  $\mu$ M) for 24 hr. Total RNA was then isolated and analyzed (10  $\mu$ g/lane) by Northern blot with indicated probes. ACC2, acetyl CoA carboxylase 2; FATP4, fatty acid transporter protein 4.

(G) Interaction of PPAR $\delta$  and PGC-1 $\alpha$  in 293 cells. Cells were transfected with HA-PPAR $\delta$  and Flag-PGC-1 $\alpha$  or Flag-PGC-1 $\alpha$ <sup>142LXXLL146</sup> motif mutant (LXXAA), then treated with vehicle or GW501516 (0.1  $\mu$ M) as indicated. HA-PPAR $\delta$  was immunoprecipitated with anti-HA affinity beads and precipitated proteins were probed with anti-flag antibodies.

(H) PGC-1 $\alpha$  coactivates PPAR $\delta$  in C2C12 muscle cells. Luciferase activity was normalized with  $\beta$ -gal activity. Shown are folds of induction calculated based on the activity from transfections without coactivator and GW501516 (first bar = 70 arbitrary units).

(I) Interaction of PPAR $\delta$  and PGC-1 $\alpha$  in gastrocnemius muscle. The nuclear extracts were incubated with protein A beads alone (lane 1), beads with PPAR $\delta$  antibodies in the absence (lane 2) or presence of GW501516 (0.1  $\mu$ M; lane 3). Precipitated proteins were probed with PGC-1 $\alpha$  antibodies. The PGC-1 $\alpha$  bands (arrow) were verified by two different PGC-1 $\alpha$  antibodies.

nally, we determined whether PPAR $\delta$  and PGC-1 $\alpha$  associate in thermogenic tissues. We isolated nuclear extracts from gastrocnemius muscle of mouse. Both PPAR $\delta$  and PGC-1 $\alpha$  protein are present in the preparations. PPAR $\delta$  antibodies coimmunoprecipitate PGC-1 $\alpha$  from the nuclear extracts (Figure 7I), suggesting an association between PPAR $\delta$  and PGC-1 $\alpha$  in vivo at physiological conditions. These results provide additional support for the hypothesis that PGC-1 $\alpha$  regulates thermogenesis at least in part through activation of PPAR $\delta$ .

## Discussion

Recent studies have uncovered distinct and tissue-restricted functions for PPAR $\gamma$  and PPAR $\alpha$ , each under-

scoring their clinical significance in metabolic disorders. In contrast, little is known for PPAR $\delta$  in lipid metabolism. Here, we demonstrate both in vivo and in vitro that PPAR $\delta$  plays a critical role in a coordinated metabolic program by upregulating fatty acid oxidation and energy expenditure.

## PPAR $\delta$ and Adipocyte Differentiation

Expression of activated PPAR $\delta$  in adipose tissue unexpectedly leads to a lean phenotype in the transgenic mice; yet these mice eat normally. This indicates that the reduction of adipose mass may occur by one of two different mechanisms: disruption of adipogenesis or elevated energy dissipation. Defects in adipogenesis typically result in irregular metabolic features such as

fatty liver, hypertriglyceridemia, and insulin resistance (Moitra et al., 1998; Shimomura et al., 1998; Barak et al., 1999). However, no components of this triad are found in the VP16-PPAR $\delta$  transgenic mice. Finally, neither activation of PPAR $\delta$  in preadipocytes *in vitro* nor targeted knockout of PPAR $\delta$  in adipose tissue *in vivo* shows any effect on adipose differentiation.

### PPAR $\delta$ in Fatty Acid Oxidation and Energy Uncoupling

Several previous studies indicate that PPAR $\delta$  may be involved in aspects of fatty acid metabolism, but its exact role and to what extent it can affect whole body physiology are not known (Leibowitz et al., 2000; Peters et al., 2000; Oliver et al., 2001; Vosper et al., 2001; Barak et al., 2002). We show here that activation of PPAR $\delta$  *in vivo* leads to systematic metabolic changes and this is achieved by elevating fatty acid catabolism and energy expenditure. Increased catabolism lowers circulating levels of triglycerides and free fatty acids and prevents adipocyte hypertrophy and lipid accumulation. Moreover, under caloric overload, activation of PPAR $\delta$  not only produces a pronounced improvement in the lipid profile, but also protects against high-fat diet- or hyperphagia-induced obesity and essentially eliminates the development of fatty liver. Consistent with these observations, key genes required for fatty acid  $\beta$ -oxidation and energy uncoupling are significantly upregulated. *In vitro*, we show that activation of PPAR $\delta$  stimulates fatty acid  $\beta$ -oxidation and triglyceride utilization in adipocytes and myotubes *in vitro*. In parallel, we observed that PPAR $\delta$ -deficient mice challenged with high-fat diet show reduced energy uncoupling and are prone to dramatic weight gain. Thus, we identify PPAR $\delta$  as a key metabolic regulator of fat burning.

Diet-induced adaptive thermogenesis is known to occur in both brown fat and muscle in response to energy overload. Metabolic activation of fat and muscle is extremely important in protection against the development of obesity. We show here that, as a dietary lipid sensor, PPAR $\delta$  links dietary status to thermogenesis. PPAR $\delta$  powerfully stimulates and coordinates at least two important aspects of this program: fuel oxidation and uncoupling. This unique function enables cells to maintain a normal cellular ATP/ADP ratio to meet the energy demands while dissipating extra energy as heat. Recent work by Spiegelman's group and others clearly established that the nuclear cofactor PGC-1 $\alpha$  is a central component of adaptive thermogenesis (Puigserver et al., 1998; Wu et al., 1999; Picard et al., 2002); however, the major target transcriptional pathway through which it mediates this effect is not known. Our data suggest that PPAR $\delta$  may be the unidentified factor. The fact that these two proteins both activate thermogenesis in the same tissues by regulating common target genes lead us to speculate that PPAR $\delta$  may employ PGC-1 $\alpha$  as its predominant coactivator in this pathway. This idea is further enforced by their induction of UCP genes in a similar cell type-selective pattern. In white fat, both PGC-1 $\alpha$  and PPAR $\delta$  induce UCP1 but not UCP2 or UCP3, whereas in muscle both induce UCP2 and UCP3, but not UCP1. We find that PGC-1 $\alpha$  is a potent coactivator for PPAR $\delta$  in muscle cells and, importantly, these

two proteins associate in thermogenic tissues *in vivo*. Taken together, we suggest that many of the thermogenic effects of PGC-1 $\alpha$  may be mediated through PPAR $\delta$ .

### PPAR Members in Lipid Metabolism: Complementary or Opposing Roles

Our work reveals interesting parallels between PPAR $\delta$  and PPAR $\alpha$ . For example, the  $\beta$ -oxidation genes induced by PPAR $\delta$  in adipose tissue largely overlap with PPAR $\alpha$  target genes in the liver. Similarly, as seen in VP16-PPAR $\delta$  transgenic mice, pharmacological activation of PPAR $\alpha$  by its agonists also lowers serum triglyceride levels. In addition, it has been shown that certain long chain fatty acids, especially polyunsaturated fatty acids, are potent activators for both PPAR $\alpha$  and PPAR $\delta$ , but are poor ligands for PPAR $\gamma$  (Forman et al., 1997). These parallels in PPAR $\alpha$  and PPAR $\delta$  responsiveness are contrasted by their distinctive patterns of expression. In particular, PPAR $\delta$  is widely expressed while PPAR $\alpha$  shows a prominent liver profile, leading to the idea that PPAR $\alpha$  and PPAR $\delta$  may act in a tissue-complementary manner. While a major role for PPAR $\alpha$  in liver is to produce ketone bodies as fuel through  $\beta$ -oxidation for peripheral tissue during fasting, PPAR $\delta$  may regulate combustion of locally available fatty acids and maintain energy balance.

In both adipose tissue and cultured adipocytes, PPAR $\delta$  and PPAR $\gamma$  appear to serve two opposing functions in fatty acid metabolism, namely catabolism versus lipogenesis and storage. In contrast to the role of PPAR $\delta$  described here, activation of PPAR $\gamma$  promotes free fatty acids influx into adipose tissue, thereby leading to increased adiposity and weight gain (Yamauchi et al., 2001b). Interestingly, recent studies suggest the existence of a similar but reversed analogy for cholesterol metabolism in macrophages. While PPAR $\delta$  promotes cholesterol accumulation in human macrophages (Vosper et al., 2001), PPAR $\gamma$  increases cholesterol efflux to protect against atherosclerosis (Li et al., 2000; Chawla et al., 2001a; Akiyama et al., 2002). These different biological effects are exerted largely by the ability of these receptors to sense different lipids along with their activation of distinct sets of target genes. We find that the PPAR $\gamma$  target genes in adipose tissue that are directly implicated in lipogenic and storage pathways are simply not induced by activation of PPAR $\delta$ . How receptors with similar DNA binding domains achieve these opposing effects is not understood.

### PPAR $\delta$ in Anti-Obesity Therapies

Obesity is a devastating medical and social problem with increasing prevalence of potentially epidemic proportions. Manipulation of adaptive thermogenesis has long been pursued to treat obesity (Spiegelman and Flier, 2001). For example, thyroid hormones stimulate thermogenesis by an uncertain mechanism and can promote weight loss, but they also produce side effects such as loss of lean body mass and cardiac toxicity. The identification of players in this pathway could create pharmacologic opportunities. Even though PGC-1 $\alpha$  and the uncoupling proteins are potential therapeutic targets, PPAR $\delta$  as a nuclear receptor, represents a bona

vide target. In particular, its ability to induce adaptive thermogenesis and protection against both dietary and genetic obesity suggests that PPAR $\delta$  agonists may be promising drug candidates for anti-obesity therapies.

#### Experimental Procedures

##### Animals

To generate VP16-PPAR $\delta$  transgenic mice, the transactivation domain (78 amino acid residues, corresponding to 413–490 residues) of VP16 was fused in frame with the N terminus of mouse PPAR $\delta$ . The VP16-PPAR $\delta$  cDNA was placed downstream of the 5.4 kb promoter/enhancer of the mouse aP2 gene (Ross et al., 1990) and upstream of the SV40 intron/poly (A) sequence. The transgene was purified and injected into C57BL/6J  $\times$  CBA F1 zygotes. Transgene positive mice were screened by Southern blot and PCR. Transgenic founder lines were backcrossed with C57BL/6J. Wild-type littermates were used as controls throughout the study. As an additional control, we also generated aP2-VP16 transgenic mice, which behave identically to wild-type animals. Null and adipose-specific PPAR $\delta$  knockout mice have been described previously (Barak et al., 2002). Mice were fed a standard chow with 4% (w/w) fat content (Harlan Teklad). For high-fat feeding, a diet containing 35% (w/w) fat content (product F3282, Bioserv) was used.

##### Histology

Tissues were fixed in 10% formalin, dehydrated, embedded in paraffin, and sectioned for haematoxylin and eosin (H&E) staining. Images were captured using Axio Vision 2.05 imaging system (Zeiss) and processed in Adobe Photoshop.

##### Ligand Treatment of *Lepr<sup>db/db</sup>* Mice

We synthesized the GW501516 compound. *Lepr<sup>db/db</sup>* mice were obtained from Jackson laboratory. GW501516 was freshly prepared in 0.5% carboxymethyl cellulose at a concentration of 4 mg/ml. Age- and weight-matched mice were treated by oral gavage either with vehicle or 10 mg/kg per day of GW501516 for 7 days. Brown fat and liver were obtained for histology analysis.

##### Analytical Procedures

Mice were fasted for 6 hr before blood was drawn. Enzymatic kits were used for measuring serum nonesterified fatty acids (Wako), total triglycerides, and total cholesterol (Sigma).

##### Northern and Western Blot Analysis and Coimmunoprecipitation Assays

PPAR $\delta$  antibodies (Affinity BioReagents Inc., and Santa Cruz Biotechnology), PGC-1 $\alpha$  antibodies (Santa Cruz Biotechnology), and VP16 antibodies (Santa Cruz Biotechnology) were purchased. Mouse EST clones were obtained from Resgen or ATCC, verified by sequencing, and used as Northern probes.

Standard protocols were used for Western and Northern blot analysis. Total tissue protein extracts (for transgene detection) and RNA were prepared with TRIzol (GIBCO-BRL) according to the manufacturer's instructions.

For coimmunoprecipitation experiments in HEK293 cells, cells in 10 cm plates were transfected using TransIT-LT1 reagent (Mirus) with plasmids encoding HA-PPAR $\delta$  and Flag-PGC-1 $\alpha$  or PGC-1 $\alpha$ <sup>142LXXLL146</sup> motif mutant (LXXAA). Next day, vehicle or PPAR $\delta$  agonist GW5015161 (0.1  $\mu$ M) was added, and cells were incubated for another 24 hr. Cells were collected in lysis buffer (50 mM Tris [pH 8.0], 200 mM NaCl, 10% glycerol, 0.5% TritonX-100, and protease inhibitors), briefly sonicated, and cleared. HA-PPAR $\delta$  was immunoprecipitated with anti-HA affinity beads and precipitated proteins were subjected to Western analysis.

To determine whether PPAR $\delta$  and PGC-1 $\alpha$  associate in vivo, nuclear extracts were isolated from gastrocnemius muscle of mouse as described (Blough et al., 1999). Nuclear proteins (300  $\mu$ g, 1  $\mu$ g/ $\mu$ l in buffer containing 20 mM HEPES [pH 7.4], 10% glycerol, 200 mM NaCl, 1.5 mM MgCl<sub>2</sub>, and 0.2 mM EDTA) were incubated with PPAR $\delta$  antibodies, then with protein A beads. Precipitated proteins were subjected to Western analysis with PGC-1 $\alpha$  antibodies.

##### Reporter Assays

C2C12 myoblasts (80% confluence) in 24-well plates were transfected using lipofectamine 2000 (Invitrogen) with 0.2  $\mu$ g PPRE-luciferase reporter, 0.2  $\mu$ g  $\beta$ -gal, 0.02  $\mu$ g PPAR $\delta$ , and 0.04  $\mu$ g indicated coactivators. Cells were treated with GW501516 as described above. Luciferase activity was normalized with  $\beta$ -gal activity. Fold of induction was calculated based on the activity from transfections without coactivator and GW501516.

##### Assays for Fatty Acid Utilization in Cultured Cells

PPAR $\delta$  and PPAR $\gamma$  adenovirus were kindly provided by Dr. W. He. VP16-PPAR $\delta$  adenoviruses were generated using the AdEasy system as previously described (He et al., 1998). The virus were purified and concentrated by cesium chloride ultracentrifugation. A multiplicity of infection of  $\sim$ 30 plaque-forming units/cell was used.

3T3-L1 preadipocytes placed in 12-well plates were cultured in Dulbecco's modified Eagle's medium (DMEM) containing 10% bovine calf serum and differentiated using standard protocols with 0.5 mM 3-isobutyl-1-methylxanthine, 0.25  $\mu$ M dexamethasone, and 5  $\mu$ g/ml insulin as inducers (Hamm et al., 2001). Differentiation of C2C12 cells into myotubes was performed with standard protocol.

For triglyceride breakdown assay, fully differentiated 3T3-L1 adipocytes were infected with virus. The next day cells were washed and serum-deprived with DMEM medium containing 2% (w/v) fatty acid-free BSA (Sigma) with or without ligands overnight. Cells were washed again and incubated in the same serum-free medium. Glycerol levels in the incubation medium were determined using a colorimetric assay (GPO-Trinder, Sigma). Cells were lysed and triglyceride (Sigma) and protein content (Bio-Rad) were determined.

For  $\beta$ -oxidation assay, 3T3-L1 preadipocytes two days postconfluence or C2C12 myotubes were either treated with ligands, or infected with virus (with or without ligands), for 30 hr. Cells were washed and incubated in low glucose DMEM medium (Catalogue #11885, GIBCO) containing 2% (w/v) fatty acid-free BSA, 0.30 mM L-carnitine, and <sup>3</sup>H-palmitic acid (3  $\mu$ Ci/well). Excess <sup>3</sup>H-palmitic acid in the medium was removed by trichloroacetic acid precipitation twice. The supernatant was extracted with chloroform:methanol (2:1) twice and then counted for <sup>3</sup>H<sub>2</sub>O production.

##### Statistical Analysis

Number of mice for each group used in experiments is indicated in the figure legends. Values were presented as mean  $\pm$  SEM. A two-tailed student's t test was used to calculate *P* values.

##### Acknowledgments

We thank Drs. W. He, Y. Barak, W. Xie, and A. Chawla for providing reagents and discussions; Dr. H. Cho for comments on the manuscript; M. Nelson, C. Bayuga, and H. Juguilon for technical help; M.A. Lawrence for histology; M. Lieberman for photography; Dr. S. Pfaff for the use of microscopes and photographic equipment; E. Stevens and E. Ong for administrative assistance. Y.-X.W. was supported by a postdoctoral fellowship from California Tobacco-Related Disease Research Program. J.H. was supported by the BK21 program, Ministry of Education, Korea. H.K. was supported by Grant 00-J-LF-01-B-78 from Critical Technology 21 on Life Phenomena and Function Research, Ministry of Science and Technology, Korea. R.M.E. is an Investigator of the Howard Hughes Medical Institute at the Salk Institute for Biological Studies and March of Dimes Chair in Molecular and Developmental Biology. This work was supported by the Howard Hughes Medical Institute.

Received: October 28, 2002

Revised: February 28, 2003

Accepted: March 7, 2003

Published: April 17, 2003

##### References

Akiyama, T.E., Sakai, S., Lambert, G., Nicol, C.J., Matsusue, K., Pimprale, S., Lee, Y.H., Ricote, M., Glass, C.K., Brewer, H.B., Jr., and Gonzalez, F.J. (2002). Conditional disruption of the peroxisome proliferator-activated receptor  $\gamma$  gene in mice results in lowered

- expression of ABCA1, ABCG1, and apoE in macrophages and reduced cholesterol efflux. *Mol. Cell. Biol.* 22, 2607–2619.
- Barak, Y., Nelson, M.C., Ong, E.S., Jones, Y.Z., Ruiz-Lozano, P., Chien, K.R., Koder, A., and Evans, R.M. (1999). PPAR $\gamma$  is required for placental, cardiac, and adipose tissue development. *Mol. Cell* 4, 585–595.
- Barak, Y., Liao, D., He, W., Ong, E.S., Nelson, M.C., Olefsky, J.M., Boland, R., and Evans, R.M. (2002). Effects of peroxisome proliferator-activated receptor  $\delta$  on placentation, adiposity, and colorectal cancer. *Proc. Natl. Acad. Sci. USA* 99, 303–308.
- Berg, A.H., Combs, T.P., Du, X., Brownlee, M., and Scherer, P.E. (2001). The adipocyte-secreted protein Acrp30 enhances hepatic insulin action. *Nat. Med.* 7, 947–953.
- Berger, J., and Moller, D.E. (2002). The mechanisms of action of PPARs. *Annu. Rev. Med.* 53, 409–435.
- Blough, E., Dineen, B., and Esser, K. (1999). Extraction of nuclear proteins from striated muscle tissue. *Biotechniques* 26, 202–206.
- Chawla, A., Boisvert, W.A., Lee, C.H., Laffitte, B.A., Barak, Y., Joseph, S.B., Liao, D., Nagy, L., Edwards, P.A., Curtiss, L.K., et al. (2001a). A PPAR $\gamma$ -LXR-ABCA1 pathway in macrophages is involved in cholesterol efflux and atherogenesis. *Mol. Cell* 7, 161–171.
- Chawla, A., Repa, J.J., Evans, R.M., and Mangelsdorf, D.J. (2001b). Nuclear receptors and lipid physiology: opening the X-files. *Science* 294, 1866–1870.
- Chen, H., Charlat, O., Tartaglia, L.A., Woolf, E.A., Weng, X., Ellis, S.J., Lakey, N.D., Culpepper, J., Moore, K.J., Breitbart, R.E., et al. (1996). Evidence that the diabetes gene encodes the leptin receptor: identification of a mutation in the leptin receptor gene in db/db mice. *Cell* 84, 491–495.
- Forman, B.M., Chen, J., and Evans, R.M. (1997). Hypolipidemic drugs, polyunsaturated fatty acids, and eicosanoids are ligands for peroxisome proliferator-activated receptors  $\alpha$  and  $\delta$ . *Proc. Natl. Acad. Sci. USA* 94, 4312–4317.
- Hamm, J.K., Park, B.H., and Farmer, S.R. (2001). A role for C/EBP $\beta$  in regulating peroxisome proliferator-activated receptor  $\gamma$  activity during adipogenesis in 3T3-L1 preadipocytes. *J. Biol. Chem.* 276, 18464–18471.
- He, T.C., Zhou, S., da Costa, L.T., Yu, J., Kinzler, K.W., and Vogelstein, B. (1998). A simplified system for generating recombinant adenoviruses. *Proc. Natl. Acad. Sci. USA* 95, 2509–2514.
- Kersten, S., Desvergne, B., and Wahli, W. (2000). Roles of PPARs in health and disease. *Nature* 405, 421–424.
- Kopecky, J., Hodny, Z., Rossmeisl, M., Syrový, I., and Kozak, L.P. (1996). Reduction of dietary obesity in aP2-Ucp transgenic mice: physiology and adipose tissue distribution. *Am. J. Physiol.* 270, E768–775.
- Lee, G.H., Proenca, R., Montez, J.M., Carroll, K.M., Darvishzadeh, J.G., Lee, J.I., and Friedman, J.M. (1996). Abnormal splicing of the leptin receptor in diabetic mice. *Nature* 379, 632–635.
- Leibowitz, M.D., Fievet, C., Hennuyer, N., Peinado-Onsurbe, J., Duez, H., Bergera, J., Cullinan, C.A., Sparrow, C.P., Baffic, J., Berger, G.D., et al. (2000). Activation of PPAR $\delta$  alters lipid metabolism in db/db mice. *FEBS Lett.* 473, 333–336.
- Li, A.C., Brown, K.K., Silvestre, M.J., Willson, T.M., Palinski, W., and Glass, C.K. (2000). Peroxisome proliferator-activated receptor  $\gamma$  ligands inhibit development of atherosclerosis in LDL receptor-deficient mice. *J. Clin. Invest.* 106, 523–531.
- Lowell, B.B., and Spiegelman, B.M. (2000). Towards a molecular understanding of adaptive thermogenesis. *Nature* 404, 652–660.
- Michalik, L., Desvergne, B., Tan, N.S., Basu-Modak, S., Escher, P., Rieusset, J., Peters, J.M., Kaya, G., Gonzalez, F.J., Zakany, J., et al. (2001). Impaired skin wound healing in peroxisome proliferator-activated receptor (PPAR) $\alpha$  and PPAR $\beta$  mutant mice. *J. Cell Biol.* 154, 799–814.
- Moitra, J., Mason, M.M., Olive, M., Krylov, D., Gavrilova, O., Marcus-Samuels, B., Feigenbaum, L., Lee, E., Aoyama, T., Eckhaus, M., et al. (1998). Life without white fat: a transgenic mouse. *Genes Dev.* 12, 3168–3181.
- Oliver, W.R., Shenk, J.L., Snaith, M.R., Russell, C.S., Plunket, K.D., Bodkin, N.L., Lewis, M.C., Winegar, D.A., Sznaidman, M.L., Lambert, M.H., et al. (2001). A selective peroxisome proliferator-activated receptor  $\delta$  agonist promotes reverse cholesterol transport. *Proc. Natl. Acad. Sci. USA* 98, 5306–5311.
- Peters, J.M., Lee, S.S.T., Li, W., Ward, J.M., Gavrilova, O., Everett, C., Reitman, M.L., Hudson, L.D., and Gonzalez, F.J. (2000). Growth, adipose, brain, and skin alterations resulting from targeted disruption of the mouse peroxisome proliferator-activated receptor  $\beta$  ( $\delta$ ). *Mol. Cell. Biol.* 20, 5119–5128.
- Picard, F., Géhin, M., Annicotte, J.-S., Rocchi, S., Champy, M.-F., O'Malley, B.W., Chambon, P., and Auwerx, J. (2002). SRC-1 and TIF2 control energy balance between white and brown adipose tissues. *Cell* 111, 931–941.
- Puigserver, P., Wu, Z., Park, C.W., Graves, R., Wright, M., and Spiegelman, B.M. (1998). A cold-inducible coactivator of nuclear receptors linked to adaptive thermogenesis. *Cell* 92, 829–839.
- Reddy, J.K., and Hashimoto, T. (2001). Peroxisomal  $\beta$ -oxidation and peroxisome proliferator-activated receptor  $\alpha$ : an adaptive metabolic system. *Annu. Rev. Nutr.* 21, 193–230.
- Rosen, E.D., and Spiegelman, B.M. (2001). PPAR $\gamma$ : a nuclear regulator of metabolism, differentiation, and cell growth. *J. Biol. Chem.* 276, 37731–37734.
- Ross, S.R., Graves, R.A., Greenstein, A., Platt, K.A., Shyu, H.L., Mellovitz, B., and Spiegelman, B.M. (1990). A fat-specific enhancer is the primary determinant of gene expression for adipocyte P2 in vivo. *Proc. Natl. Acad. Sci. USA* 87, 9590–9594.
- Shimomura, I., Hammer, R.E., Richardson, J.A., Ikemoto, S., Bashmakov, Y., Goldstein, J.L., and Brown, M.S. (1998). Insulin resistance and diabetes mellitus in transgenic mice expressing nuclear SREBP-1c adipose tissue: model for congenital generalized lipodystrophy. *Genes Dev.* 12, 3182–3194.
- Spiegelman, B.M., and Flier, J.S. (2001). Obesity and the regulation of energy balance. *Cell* 104, 531–543.
- Steppan, C.M., Bailey, S.T., Bhat, S., Brown, E.J., Banerjee, R.R., Wright, C.M., Patel, H.R., Ahima, R.S., and Lazar, M.A. (2001). The hormone resistin links obesity to diabetes. *Nature* 409, 307–312.
- Tan, N.S., Michalik, L., Noy, N., Yasmin, R., Pacot, C., Heim, M., Fluhmann, B., Desvergne, B., and Wahli, W. (2001). Critical roles of PPAR $\beta$ / $\delta$  in keratinocyte response to inflammation. *Genes Dev.* 15, 3263–3277.
- Vosper, H., Patel, L., Graham, T.L., Khoudoli, G.A., Hill, A., Macphee, C.H., Pinto, I., Smith, S.A., Suckling, K.E., Wolf, C.R., and Palmer, C.N. (2001). The peroxisome proliferator-activated receptor  $\delta$  promotes lipid accumulation in human macrophages. *J. Biol. Chem.* 276, 44258–44265.
- Wu, Z., Puigserver, P., Andersson, U., Zhang, C., Adelmant, G., Mootha, V., Troy, A., Cinti, S., Lowell, B., Scarpulla, R.C., and Spiegelman, B.M. (1999). Mechanisms controlling mitochondrial biogenesis and respiration through the thermogenic coactivator PGC-1. *Cell* 98, 115–124.
- Yamauchi, T., Kamon, J., Waki, H., Terauchi, Y., Kubota, N., Hara, K., Mori, Y., Ide, T., Murakami, K., Tsuboyama-Kasaoka, N., et al. (2001a). The fat-derived hormone adiponectin reverses insulin resistance associated with both lipoatrophy and obesity. *Nat. Med.* 7, 941–946.
- Yamauchi, T., Kamon, J., Waki, H., Murakami, K., Motojima, K., Komeda, K., Ide, T., Kubota, N., Terauchi, Y., Tobe, K., et al. (2001b). The mechanisms by which both heterozygous peroxisome proliferator-activated receptor  $\gamma$  (PPAR $\gamma$ ) deficiency and PPAR $\gamma$  agonist improve insulin resistance. *J. Biol. Chem.* 276, 41245–41254.